

Published in final edited form as:

J Exp Zool B Mol Dev Evol. 2011 December 15; 316(8): 547–561. doi:10.1002/jez.b.21430.

Effects of environmental perturbations during postnatal development on the phenotypic integration of the skull

Paula Natalia Gonzalez^{1,*}, Evelia Edith Oyhenart², and Benedikt Hallgrímsson¹

¹Department of Cell Biology and Anatomy, University of Calgary. 3280 Hospital Drive NW, Calgary, AB, Canada T2N 4Z6

²Instituto de Genética Veterinaria. Facultad de Ciencias Veterinarias, UNLP-CCT La Plata, CONICET. 60 and 118 S/N, La Plata, Buenos Aires, Argentina 1900

Abstract

Integration and modularity are fundamental determinants of how natural selection effects evolutionary change in complex multivariate traits. Interest in the study of the specific developmental basis of integration through experimental approaches is fairly recent and it has mainly focused on its genetic determinants. Here we present evidence that postnatal environmental perturbations can modify the covariance structure by influencing the variance of some developmental processes relative to the variances of other processes that contribute to such structure. We analyzed the effects of the reduction of nutrient supply in different ontogenetic stages (i.e., before and after weaning, and from birth to adulthood) in *Rattus norvegicus*. Our results show that this environmental perturbation alters the phenotypic variation/covariation structure of the principal modules of the skull (base, vault and face). The covariance matrices of different treatment groups exhibit low correlations and are significantly different, indicating that the treatments influence covariance structure. Postnatal nutrient restriction also increases the variance of somatic growth. This increased variance drives an increase in overall integration of cranial morphology through the correlated allometric effects of size variation. The extent of this increase in integration depends on the time and duration of the nutritional restriction. These results support the conclusion that environmental perturbations can influence integration and thus covariance structure via developmental plasticity.

Keywords

developmental plasticity; stress; modularity; 3 dimensional geometric morphometrics; *Rattus norvegicus albinus*

Morphological variation arises through variation in developmental processes including pattern formation, differentiation, growth, pattern formation and epigenetic interactions among component parts (Atchley and Hall, '91). Developmental processes act at many levels, from the molecular and cellular levels that involve signaling interactions and cell behaviour such as division, death and migration, to higher levels that comprise functional

*Correspondence to: Paula N. Gonzalez Department of Cell Biology and Anatomy, University of Calgary. 3280 Hospital Drive NW, Calgary, AB, Canada T2N 4Z6. Phone: 587-580-7258. Fax: 403-210-9573. pgonzale@ucalgary.ca; paulan.gonza@gmail.com.

interactions among tissues and organs, somatic growth, among others (Hall, 2003; Salazar-Ciudad et al., 2003). Such processes have the potential to generate integration at the phenotypic level, which refers to the tendency to express coordinated variation among traits (Willmore et al., 2007; Hallgrímsson et al., 2009). This property of developmental systems is essential for understanding evolutionary change, since it determines the structure of variation generated given different genetic and environmental perturbations (Hendrikse et al., 2007). Covariance structure is a fundamental determinant of how natural selection effects the evolutionary change in complex multivariate traits (Lande, '79) and thus of evolvability.

Interest in phenotypic integration is not new in evolutionary studies, but interest in the study of the specific developmental determinants of integration through experimental approaches is fairly recent (Mitteroecker et al., 2005; Hallgrímsson et al., 2006; Hallgrímsson and Lieberman, 2008). The main reason for taking this approach is that the developmental determinants of integration cannot be reliably inferred from phenotypic covariance patterns alone. The relationship between phenotypic covariation and integration can be obscured by the superimposition of multiple determinants of covariance in complex systems and the dependence of covariation structure on variances in covariance-generating processes (Hallgrímsson et al., 2009). For this reason, several recent studies have manipulated genetic and environmental factors in order to infer the developmental basis for morphological integration, particularly in the mammalian skull (Willmore et al., 2006; Hallgrímsson et al., 2007a; Gonzalez et al., 2011). In addition, the controlled induction of specific perturbations allows the evaluation of how the properties of development systems modulate the ways in which anatomical structures can vary in response to different genetic and environmental factors (Badyaev and Foresman, 2000; Pigliucci and Hyden, 2001; Hallgrímsson et al., 2007b; Gonzalez et al., 2011). Previous studies aimed at evaluating if cranial integration patterns the effects of genetic variation have shown that the skull is a highly integrated structure whose covariation is predictably structured, and thus genetic perturbations that influence the size and shape of particular units will have unequal but consistent effects on other regions of the skull (Hallgrímsson et al., 2007b). In a similar way, Badyaev and Foresman (2000) determined that the pattern of integration of the mandible can modulate the stress-induced changes. By growing *Sorex* shrew species under stressful conditions, they found that variation in mandibular shape was not uniformly distributed but confined to less-integrated traits.

While previous work has mainly focused on genetic determinants of covariation structure, environmental perturbation can also influence covariance structure in several ways. In developmental terms, this can occur if environmental perturbations introduce new variation by influencing the variance of a developmental process relative to the variances of other processes that contribute to covariance structure (Hallgrímsson et al., 2009). Such processes can be temporally patterned but also spatially arranged in the sense that they differentially influence components of a complex morphological structure. Increased variance of some developmental process will result in an increase of phenotypic integration if the process that is affected produces a highly correlated response and if the developmental process affected is a major contributor to covariance structure. Conversely, a developmental perturbation that

introduces a new source of variation or one that increases the variance of a process that is not normally a major contributor to covariance structure will produce a disintegrating response.

Herein we examine the effects of restricting the nutrient supply during postnatal development on phenotypic variation and covariation structure of the skull in a rat model. Nutrition is one of the main factors controlling organismal growth through the modulation of synthesis and secretion of insulin-like signaling molecules (Nijhout, 2003). Although the pathways by which this takes place are incompletely understood, existing reports show that malnutrition results in a reduction of overall cranial size and that some components, such as facial structures, seem to be more affected than others (Pucciarelli '80; Dahinten and Pucciarelli, '86; Dressino and Pucciarelli, '96; Miller and German, '99; Oyhenart et al., '98, 2003). Such differences are expected since the skull of all vertebrates is not a single developing unit but a complex structure that comprises recognizable parts that are coherent according to their developmental origin, structure, and function. These parts can be thought of as modules in the sense that they are highly integrated by numerous and usually strong interactions while the interactions among them are relatively weaker (Cheverud, '82, '89, '96; Lieberman et al., 2000; Hallgrímsson et al., 2004; Klingenberg, 2008). To date, however, little is known about how the modifications of somatic growth induced by environmental perturbations affect the pattern of interactions between cranial traits.

Based on the studies discussed above we propose a set of hypotheses about the effects of postnatal nutrient restriction on the mammalian skull. First, we expect that nutrient restriction reduces skull size through reduction of somatic growth. However, due to allometry, we predict that this relatively generalized effect will differentially affect the growth of the three main modules (i.e. base, face and vault) of the skull (Cheverud, '82; Sperber, 2001; Morris-Kay and Wilkie, 2005; Mitteroecker and Bookstein, 2007). In particular, we predict that the effect of growth reduction will be greater in the face than in the neurocranium (vault and base). This prediction is based on two considerations. The first is that the neurocranium grows earlier than the face. The neurocranium will thus have proportionately less growth remaining during the period at which we administer the nutritional stress. The second reason is that neurocranial growth is closely related to brain growth and the brain tends to be at the expense of other growth components (Baker et al., 2010). Secondly, we predict that the differential effects of nutritional restriction of cranial components will produce an alteration of covariance structure. This will occur because the differential effects of growth restriction on the components of the skull will alter the covariances among them. If the variance of growth is also increased, we further predict that morphological integration will be increased by this environmental stress. The alternative and null hypothesis is that all the structures are equally affected by the alteration of somatic growth. In that case, neither covariance structure nor integration will be influenced by the treatments.

MATERIALS AND METHODS

Animals

The animals used in this study were *Rattus norvegicus albinus*, var. Wistar, brought from the Comisión Nacional de Energía Atómica (Argentina) in 1997. They were maintained as an outbred colony in the animal house of the Instituto de Genética Veterinaria (IGEVET, Universidad Nacional de La Plata, Argentina). The animals were kept free of pathogens and treated in compliance with standardized institutional guidelines. Rats were housed in solid stainless steel cages (12" × 12" × 6.8"), which were cleaned three times a week. The room temperature ranged from 21 to 25°C and the photoperiod was 12h of light, from 6:00 a.m. to 6:00 p.m. They were fed on a pelleted and sterilized commercial stock diet containing proteins (23%), carbohydrates (44%), lipids (11%), water (8%), fiber (5%), mineral mixture (3%) and vitamin mixture (1%).

Experimental design

Fifty adult female rats were mated overnight with ten adult males. Pregnancy was assumed to start after spermatozoa were found in the vaginal smear. Pregnant rats were housed in individual steel boxes, and fed on stock diet and water *ad libitum*. At delivery, dams and their pups were submitted to one of the following treatments: Control (C): dams and their pups received stock diet *ad libitum*; Early Malnutrition (EM): during lactation dams were pair-fed half the amount of stock food consumed by the weight-matched control rats; after weaning and until the end of the experiment (63 days old) the pups were fed on stock diet *ad libitum*; Late Malnutrition (LM): dams received stock diet *ad libitum* and their pups were fed on a low protein diet (2%) after weaning throughout; Total Malnutrition (TM): during lactation dams were pair-fed half the amount of stock food consumed by the weight-matched control rats, and the pups received a low protein diet (2%) after weaning throughout. The litters of the four treatments were weaned at the same age (21 days) and separated by sex. Food intake was measured daily and body weight was measured every 3 days from birth to weaning, then the animals were weighed once a week up to 63 days of age. Animals were euthanized by cervical dislocation, following approved standard operating procedures.

Finally, the sample was composed as follows: C: 15 males and 15 females; EM: 21 males and 18 females; LM: 11 males and 16 females; and TM: 8 males and 12 females.

Data collection

All crania were micro CT-scanned (Scanco Viva-CT40, Scanco Medical AG, Basserdorf, Switzerland) at 35 µm resolution (70 kv, 160 mA, 500 projections). Sixty two three-dimensional (3D) landmarks from both sides of the skull (Fig. 1, Table 1) were digitized using Analyze 5.0 (Biomedical Imaging Resource 2003). Landmarks were assigned to three skull modules: base, face and vault.

Each specimen was digitized two times on separate days by the same observer in order to assess measurement error. We compared statistically the coordinates obtained in the two series using the intra-class correlation coefficient and repeated measures ANOVA. The results showed no significant levels of error in the placement of landmarks.

We used geometric morphometrics based on Procrustes superimposition to characterize size and shape variation (Bookstein, '91). Data used for all analyses were aligned by means of the Procrustes generalized least squares method using MorphoJ (Klingenberg, 2011). This procedure optimally translates, scales and rotates coordinates of landmarks (Rohlf and Slice, '90). The symmetric component of each module was extracted and the resulting coordinates were used as shape variables. The symmetric component for each specimen was obtained estimating the average of the left and right configurations (Klingenberg, 2002). This procedure resulted in 16 landmarks for the base and the face, and 8 landmarks for the vault. As a measure of overall size, we computed centroid size, which is the square root of the sum of squared distances of each landmark coordinate from the centroid (mean x, y, z, landmark for the configuration) of the configuration. The centroid size of the specimens was measured for each data set and was used to scale the raw coordinates in the Generalized Procrustes Superimposition (Bookstein, '91).

Statistical analyses

The effect of environmental perturbations on the overall growth was evaluated by comparing the mean body weight among groups at 63 days. We also performed a Levene's test to compare the magnitude of within-group variation in body weight among groups. A nonlinear Gompertz model was fitted to the ontogenetic trajectory of body weight in order to obtain an estimate of the final size attained by each group, which is summarized by the asymptote of the model (Ritz and Streibig, 2008). The interval of confidence for the asymptote was obtained by bootstrap (n=999).

Differences in mean size of skull components between groups were investigated by a one-way analysis of variance. The amount of variance in the size of skull components within each group was compared using Levene's test.

The patterns of shape differentiation in the skull were investigated using a principal component analysis (PCA) on the variance-covariance (VCV) matrix, a method used to describe the major axes of shape variation in a sample. In addition, a separate Procrustes superimposition of the raw regional 3D landmarks of each module was performed. Visualizations of shape changes were performing by warping the scanned surface of a rat skull, using the thin-plate spline procedure implemented by Landmark software (Wiley et al., 2005). Deformations of wireframes were also used to visualize the differences in shape along the first two principal components using MorphoJ (Klingenberg, 2011). Among-individual variance in shape for each group was estimated as the within group Euclidean distances along the entire set of PCs. The homogeneity of variances among groups was further evaluated with Levene's test.

For quantifying overall similarity in the structure of association among traits we calculated the correlation between covariance matrices (Mantel, 1967). Although correlation matrices among phenotypic traits are also used, within geometric morphometrics covariance matrices are consistently used because the landmark coordinates affect the way matrix correlations are computed (Klingenberg et al., 2002; Klingenberg, 2011). The computation of correlation matrices involves a different scaling of each variable, which would result in a different scaling of each landmark coordinate and a distortion of the geometry of the landmark

configuration. The matrix correlation is the Pearson correlation computed using the corresponding elements of the two matrices as paired observations and measures the strength of association between them. A correlation of +1 indicates that the covariation patterns are equal or proportional. A correlation of zero indicates unrelated structure between the matrices, and a correlation of -1 specifies matrices that are mirror images (Roff, 2000; Marroig and Cheverud, 2001).

To test the association statistically, we use a procedure specially adapted for the comparison of covariances matrices derived from coordinates of landmarks, which takes into account the fact that the x , y and z coordinates of landmarks are interdependent (Klingenberg and McIntyre, '98; Klingenberg et al., 2002). In this analysis, the landmarks, instead of the coordinates, are permuted in the covariance matrices; this maintains the association between the coordinates of each landmark. The permutation procedure was carried out 10,000 times. For each iteration, the landmarks were permuted for one matrix and its correlation to the other matrix was computed. The resulting null distribution was compared to the matrix correlation calculated for the original pair of matrices.

Matrix correlations were then adjusted to account for small sample size following Marroig and Cheverud (2001), using the formula $R_{adj} = R_{obs}/R_{max}$. Maximum matrix correlation (R_{max}) was estimated using the formula $R_{max} = (t_{atb})^{1/2}$. To estimate covariance matrix repeatability (t), the original datasets were resampled and covariance matrices re-estimated 1000 times, and the mean matrix correlation between these and the original datasets was taken as an estimate of t (Marroig and Cheverud, 2001).

We calculated an integration index based on the variance of the eigenvalues of the covariance matrices (Wagner, '90; Pavlicev et al., 2009). This index is based on the fact that the eigenvalues of a matrix give the amount of variance associated with the corresponding eigenvector. If there are only a few eigenvalues that are large compared to the rest of the eigenvalues, then the variation of the characters is more or less confined to the few corresponding eigenvectors (Wagner, '90). We corrected for differences in sample variance by scaling the variance of eigenvalues to the mean eigenvalue. In addition, to account for the dependency on the size of the matrix when eigenvalue variance is compared among matrices, we estimated the relative eigenvalue variance by dividing the observed eigenvalue variance by the maximum eigenvalue variance for the particular number of traits (Pavlicev et al., 2009). Partial indices of integration for the three cranial modules were calculated using this method.

To study size-related shape changes within treatments we performed a multivariate regression of the Procrustes coordinates on log centroid size (Monteiro, '99). The amount of variation accounted by the regression model was quantified as a percentage of the total shape variation, computed using the Procrustes metric. The statistical significance of the regressions was evaluated with permutation tests against the null hypothesis of independence. For comparisons between within-group allometries we calculated Pearson's product-moment correlation coefficient between regression vectors. The correlation values were compared to the distribution of values generated by bootstrap resampling ($n=999$). Then, we calculated the arccosine of the signed inner products between the regression

vectors to obtain the angles between the regression vectors. A right angle is expected for pairs of random vectors, which means that allometric trajectories of the samples under comparison are not parallel and thus, they differ in the pattern of shape changes related with size (Cardini and Thorington, 2006; Drake and Klingenberg, 2008; Gonzalez et al., 2010).

The statistical analyses were performed using MorphoJ (Klingenberg, 2011) and R 2.10.0 (R Development Core Team, 2009).

RESULTS

Malnutrition produces a significant reduction of body weight in the three treatments both in females and males (Table 2). Comparison of variances for body mass by Levene's test revealed that the LM and TM groups showed a significant reduction in the variance of body size attained at 63 days old. The EM group showed a significant increase in its variance. The maximum body weight estimated by the asymptote of the Gompertz model was also lower in the three treatments than in the Control group. Figure 2 displays the longitudinal data for body weight and the adjusted Gompertz model by treatment and sex.

Table 3 summarizes the mean values of size (CS) for the three skull components and their standard deviation by group. The three treatments showed significant reduction in size compared with the Control group. Proportional average reduction from control size was greater for LM and TM groups for the face component. Conversely, the EM group showed greater reduction for the vault than for the other two components. The ANOVA test indicated the existence of significant differences in size among treatments for the three modules. The two post hoc tests performed, Tukey and Bonferroni, showed that most pairwise comparisons were significant at $P < 0.01$, except between the Late-Total Malnutrition comparison. Levene's test showed higher among-individual variance in size in the EM group for the three components analyzed.

The first principal component (PC1) extracted from the whole skull accounts for 61.20% of the total variance, and it separates the Control group from the LM and TM groups. The second component accounts for a small proportion of total variance (8.88%) and it separates Control and EM groups. Variation along PC1 is manifested primarily in the breadth of the vault and the base, and the length of the face (Fig. 3). In contrast, variation along PC 2 is mainly manifested in the breadth of the face. Similar shape changes can be observed when the three skull modules are analyzed separately (Figs. 4 A, B, C).

The distribution of individuals along the first two principal components suggests that EM group shows a greater variation in shape. Within group Euclidean distances along the entire set of PCs is larger for the EM group in the three components analyzed (Fig. 5). Disparity of within group variance in shape between treatments was further confirmed by Levene's test ($P < 0.01$).

The matrix correlations between covariance matrices for each treatment are presented in Table 4. Correlation values varied between 0.283 and 0.649, and all were significant ($P \leq 0.01$). Matrix repeatability ranges from 0.883 to 0.920 in the base, from 0.890 to 0.914 in the face and finally, from 0.842 to 0.931 in the vault. Accordingly, maximum values of

correlation expected range from 0.848 to 0.907. Adjusted matrix correlations between treatments range from 0.315 to 0.737. The highest correlation values between the VCV matrices were found between LM and TM groups, whereas the lowest values were found between the Control group and the other three treatments (Table 4).

The patterns of the scaled variance of the eigenvalues as a measure of integration show an increase in integration for the EM group, especially for the base and vault (Fig. 6). Conversely, compared to Control and MR groups, the LM and TM groups display lower values of integration for the base. A similar pattern was found by comparing the level of integration using the relative variance of eigenvalues (Table 5).

The multivariate regressions of Procrustes coordinates on centroid size within treatments were statistically significant ($P < 0.01$) and showed that centroid size accounted for 8 to 32% of the total shape variation, depending on the cranial unit and the group analyzed. The largest values were obtained for the EM group, with values of 24.454% for the vault, 32.238% for the face and 29.177% for the base. The Control group exhibited a similar amount of shape variation accounted by size in the three skull components analyzed; with the largest value also obtained for the face (16.601%) compared to the vault (12.341%) and the base (12.239%). The other two groups (LM and TM) exhibited values ranging from 8.199% to 20.255%. Regarding the skull components, the face showed larger values of shape variation explained by size than the other two components for all the groups analyzed. These results suggest that a large percentage of skull shape variation within samples is independent of size.

The pattern of size-related shape changes within group for the LM and TM groups differs significantly from Control for the base and face. Pairwise comparisons between regression vectors of static allometry show low values of correlation not significant statistically (Table 6). This means that the angles between regression vectors were not significantly different from the expected right angle for pairs of random vectors. The highest correlation values were found between the three malnourished groups for three skull components analyzed. These results are similar to those obtained for the correlation between covariance matrices derived from Procrustes superimposed data, although the comparison of regression vectors only contains information about the fraction of shape that covaries with size.

Discussion

As predicted, the reduction of nutrient supply altered the growth, as is shown by the smaller body and skull size attained by the malnourished groups (Tables 2, 3). Based on developmental and functional data considerations, we expected that the nutrient restriction would differentially affect the growth of the three modules and that this differential effect would alter covariation structure. In particular, we predicted a larger reduction of growth in the facial component than in the neurocranium. All three components were significant smaller in the malnourished groups. Interestingly, however, the pattern of size decrease was related to the ontogenetic period in which the perturbation was induced. When the period of starvation persisted until adulthood, the face was the component with the largest decrease in size. A similar response of the viscerocranium to low protein and caloric diets has been

previously documented in rodents and primates (Dressino and Pucciarelli, '97; Miller and German, '99; Oyhenart et al., 2003). Conversely, when the diminution of nutrient supply only occurred during the early part of ontogeny, i.e. from birth to weaning, the vault was the component most affected, showing a reduction of 12% compared to controls, while the face and the base were reduced in a 7% and 8%. We infer that differences in response are due to differences in the timing of growth between the modules analyzed. Vault growth is strongly influenced by the development of the brain, which occurs earlier than other structures in the skull (Geoffrey, 2001). As a consequence, this component displays a high rate of growth during the early ontogeny and a shorter period of postnatal growth. While the vault displays a faster deceleration between birth and weaning (Hughes et al., '78), facial growth extends for a longer period and a larger percentage of its final size is normally attained after weaning. This means that when food consumption was restored in the EM group, the facial component was normally growing at a higher velocity than the vault. Such difference could account for the greater reduction in vault size with respect to facial size that was observed in this group.

Comparisons of skull shape also revealed large differences between the three treatments and the control group. The main shape changes associated with the reduction of nutrient supply, extracted from the first PC, were characterized by an anteroposterior shortening of the skull and a relative increase of the skull breadth. These results suggest that morphological changes in response to stressors occurred along a direction of ontogenetic variation (West-Eberhard, 2003; Young and Badyaev, 2010). The broad pattern of shape change that we see between control and malnourished groups mimics that of postnatal ontogenetic shape change in the skull of rodents as well as other mammals. In particular, there is an ontogenetic lengthening of the skull with age due to the predominant anteroposterior direction of facial growth (Dressino and Pucciarelli, '97; Miller and German, '99; Gonzalez et al., 2011). A similar pattern of phenotypic variation, where larger crania tend to have longer vaults and faces compared to smaller crania, has been observed among natural populations of modern humans and primates (Marroig, 2007; Perez and Monteiro, 2009; Perez et al., 2011). These results suggest that, although the particular environmental and genetic causes of size variation at intra and inter-specific levels can be different, they might have similar consequences in cranial shape due to the contribution of the same developmental processes.

We also hypothesized that nutrient restriction would produce a generalized alteration in covariance structure. We found relatively low correlations between the covariance matrices of each module of among treatments, indicating that integration pattern were indeed altered by nutrient restriction. The lowest values were found in the face with correlation values ranging from 0.316 to 0.372. Previous studies aimed at evaluating the effect of mutations on the covariance pattern of the skull have noted that low correlations among covariance matrices are to be expected when the phenotypic variances for the traits in the matrix are low (Hallgrímsson et al., 2007; Jamniczky and Hallgrímsson, 2009). In such cases even small genetic changes can result in large alterations of the variance of covariance-generating processes in the development of organismal form. Our results suggest that environmentally induced changes can also have such an effect on covariance matrices. Although this plasticity in the pattern of integration among phenotypic traits has not been analyzed thoroughly, there are well supported reasons to expect that in multivariate phenotypes,

environmental conditions induce not only variation in individual traits, but also differences in the integration among traits (Schlichting, '89a,b; Pigliucci, 2001, 2004).

It is well known that the restriction of nutrient supply affects overall determinants of growth, such as the activity of several hormones and factors that play an important role in regulating organism growth (Thissen et al., '94; Nijhout, 2003; Martin et al., 2005; Kappeler et al., 2009). Moreover, a recent study has demonstrated that the nutritional status in early life might induce permanent modifications on hormone activity in adults, associated with changes of the GH/IGF-I endocrine axis (Kappeler et al., 2009). The alteration of such common growth factors mediates the overall size reduction observed in malnourished individuals. However, the low correlation values between covariance matrices of Control and treatments suggest that local determinants of growth (e.g. autocrine/paracrine IGF-I; Le Roith et al., 2001) drove specific and local responses to systemic factors in the cranial structures analyzed. This is further supported by the differences found in the static allometry of the base and face between the control group and the two groups with extended starvation (LM-TM), which indicates that the pattern of covariation of shape with size was altered. These findings stress the importance of local factors in mediating the changes in the covariation structure under different environmental or genetic perturbations (Hallgrímsson and Lieberman, 2008; Mitteroecker and Bookstein, 2008).

Environmental perturbations are thought to increase the phenotypic variance within groups (Badyaev, 2005; Jones and German, 2005). For nutritional stress, we report here that the time and duration of the nutritional stress influences the extent of the effect on the within-group variance. The restriction of nutrients during lactation led to a larger variation in the phenotypic traits under study (i.e. body weight, and size and shape of cranial modules). In contrast, the traits of the two groups under extended malnutrition showed either similar values or a significant reduction in their variation compared to the Control group. Previous studies have also reported that variation of different traits responds differentially to unfavorable environmental conditions (e.g., Stanton et al., 2000; Cesani Rossi et al., 2006). The nonlinearity between the strength of nutritional restriction and the phenotypic variation reported in this study may reflect underlying nonlinearities in the relation between complex traits and their genetic, environmental and developmental determinants (Klingenberg and Nijhout, '99; Gilchrist and Nijhout, 2001; Nijhout, 2002). If individuals vary in their response to nutritional stress, then the magnitude of the variance in the response will depend on the growth velocities of particular structure at the time of the environmental perturbation. Individuals can also vary in their capacity for catch-up subsequent to the stress period which further complicates this relationship.

Finally, we expected that changes in the variance of somatic growth would result in alterations in the level of phenotypic integration in cranial traits. Particularly, in the case of nutritional deficiency, variation in the degree to which individuals exhibit a reduction in growth results in a source of covariation that is not present in a population in which no individuals exhibit a reduction in growth due to poor nutrition. Previous studies have shown that changes in variance in covariance-generating developmental processes can produce radically different covariance structures and increase or decrease overall integration depending on the relative importance of the process under study in determining covariance

structure (Hallgrímsson et al., 2009). Accordingly, we observed that in the EM group the increased variance in the growth of the three components of the skull, inferred from the variance in size, resulted in an increase in the morphological integration as measured by the scaled and relative variances of eigenvalues. As somatic growth is a major contributor to cranial covariation, due to the allometric effects of growth, increasing its variance also increases the magnitude of correlated responses driven by this process.

The results reported in this study reveal the influence of environmental factors on the variance-covariance structure of the skull. The evidence presented here indicates that both the pattern and magnitude of phenotypic integration of the skull are affected by the alteration of somatic growth induced by the reduction of nutrient supply. Furthermore, we found that the specific responses depend on the time and magnitude of the environmental perturbation induced. These morphological changes in skull components are probably mediated by the action of both general and local factors. However, we have only a very limited understanding of the mechanisms that control size and associated shape variation in specific tissues. Further work in this direction is required to ascertain how tissue-specific responses within structures are produced under the influence of common external factors. We believe that approaches that focus on the influence of particular developmental processes in controlled experimental contexts have the potential to unravel the intricate relationship between phenotypic variation in complex traits and their genetic and environmental determinants.

Acknowledgments

We thank Wei Liu for technical assistance. This study was funded by the Consejo Nacional de Investigaciones Científicas y Técnicas and the Universidad Nacional de La Plata (P.N.G and E.E.O), the CIHR Training Program in Genetics, Child Development of the Health Alberta Children's Hospital Research Institute for Child, Maternal Health and a fellowship award from Alberta Innovates Health Solutions (P.N.G) and National Science and Engineering Council (NSERC), Canadian Foundation for Innovation, Alberta Innovation and the University of Calgary grants to B.H.,.

References

- Atchley WR, Hall BK. A model for development and evolution of complex morphological structures. *Biol Rev.* 1991; 66:101–157. [PubMed: 1863686]
- Badyaev AV, Foresman KR. Extreme environmental change and evolution: stress-induced morphological variation is strongly concordant with patterns of evolutionary divergence in shrew mandibles. *Proc R Soc Lond B.* 2000; 267:371–377.
- Badyaev, AV. Role of Stress in Evolution: From Individual Adaptability to Evolutionary Adaptation. In: Hallgrímsson, B.; Hall, BK., editors. *Variation. A central concept in biology.* New York: Academic Press (Elsevier); 2005. p. 277-302.
- Baker J, Workman M, Bedrick E, Frey MA, Hurtado M, Pearson O. Brains versus brawn: An empirical test of Barker's brain sparing model. *Am J Hum Biol.* 2010; 22:206–215. [PubMed: 19701887]
- Bookstein, FL. *Morphometric Tools for Landmark Data: Geometry and Biology.* Cambridge: Cambridge University Press; 1991.
- Calvanti, MJ. Mantel for windows, Version 1.18. ckwel Publishing Ltd; 2008. Freeware available at <http://life.bio.sunysb.edu/morph/>.
- Cesani MF, Orden AB, Oyhenart EE, Zucchi M, Muñe MC, Pucciarelli HM. Growth of functional cranial components in rats submitted to intergenerational undernutrition. *J Anat.* 2006; 209:137–147. [PubMed: 16879595]

- Cheverud J. Phenotypic, genetic, and environmental morphological integration in the cranium. *Evolution*. 1982; 36:499–516.
- Cheverud, J. Trends in Vertebrate Morphology, Proceedings of the 2nd International Symposium on Vertebrate Morphology, Fortschritte der Zoologie. Vol. 35. New York: Gustav Fisher Verlag; 1989. Evolution of morphological integration; p. 196-197.
- Cheverud JM. Developmental integration and the evolution of pleiotropy. *Am Zool*. 1996; 36:44–50.
- Dahinten S, Pucciarelli HM. Variations in sexual dimorphism in the skulls of rats subjected to malnutrition, castration, and treatment with gonadal hormones. *Am J Phys Anthropol*. 1986; 71:63–67. [PubMed: 3777148]
- Dressino V, Pucciarelli HM. Efecto nutricional sobre el crecimiento craneofacial de *Saimiri sciureus* (Cebidae). Un estudio experimental. *Rev Arg Antrop Biol*. 1996; 1:98–112.
- Dressino V, Pucciarelli HM. Cranial growth in *Saimiri sciureus* (Cebidae) and its alteration by nutritional factors: A longitudinal study. *Am J Phys Anthropol*. 1997; 102:545–554. [PubMed: 9140543]
- Gilchrist MA, Nijhout HF. Nonlinear developmental processes as sources of dominance. *Genetics*. 2001; 159:423–432. [PubMed: 11560916]
- Gonzalez PN, Hallgrímsson B, Oyhenart E. Developmental plasticity in the covariance structure of the skull: effects of prenatal stress. *J Anat*. 2011; 218:243–257. [PubMed: 21138433]
- Hall BK. Evo-Devo: evolutionary developmental mechanisms. *Int J Dev Biol*. 2003; 47:491–495. [PubMed: 14756324]
- Hallgrímsson B, Lieberman DE. Mouse models and the evolutionary developmental biology of the skull. *Int Comp Biol*. 2008; 48:373–384.
- Hallgrímsson B, Willmore K, Dorval C, Cooper DML. Craniofacial variability and modularity in macaques and mice. *J Exp Zool (Mol Dev Evol)*. 2004; 302:207–225.
- Hallgrímsson B, Brown JY, Ford-Hutchinson AF, Sheets HD, Zelditch ML, Jirik FR. The brachymorph mouse and the developmental-genetic basis for canalization and morphological integration. *Evolution & Development*. 2006; 8:61–73. [PubMed: 16409383]
- Hallgrímsson B, Lieberman DE, Liu W, Ford-Hutchinson AF, Jirik FR. Epigenetic interactions and the structure of phenotypic variation in the cranium. *Evol Dev*. 2007a; 9:76–91. [PubMed: 17227368]
- Hallgrímsson, B.; Lieberman, DE.; Young, NM.; Parsons, T.; Wat, S. Evolution of covariance in the mammalian skull. In: Bock, G.; Goode, J., editors. *Tinkering - The Microevolution of Development* (Novartis Found Symp 284). 2007b. p. 164-190.
- Hallgrímsson B, Jamniczky H, Young N, Rolian C, Parsons T, Boughner J, Marcucio R. Deciphering the palimpsest: studying the relationship between morphological integration and phenotypic covariation. *Evol Biol*. 2009; 36:355–376. [PubMed: 23293400]
- Hendrikse JL, Parsons TE, Hallgrímsson B. Evolvability as the proper focus of evolutionary developmental biology. *Evol Dev*. 2007; 9:393–401. [PubMed: 17651363]
- Hughes PCR, Tanner JM, Williams JPG. A longitudinal radiographic study of the growth of the rat skull. *J Anat*. 1978; 127:83–91. [PubMed: 701198]
- Jamniczky HA, Hallgrímsson B. A comparison of covariance structure in wild and laboratory murid crania. *Evolution*. 2009; 63:1540–1556. [PubMed: 19210537]
- Jones, DC.; German, RZ. Variation in Ontogeny. In: Hallgrímsson, B.; Hall, BK., editors. *Variation. A central concept in biology*. New York: Academic Press (Elsevier); 2005. p. 71-85.
- Kappeler L, De Magalhaes Filho C, Leneuve P, Xu J, Brunel N, Chatziantoniou C, Le Bouc Y, Holzenberger M. Early postnatal nutrition determines somatotrophic function in mice. *Endocrinology*. 2009; 150:314–323. [PubMed: 18801897]
- Klingenberg CP. Morphological integration and developmental modularity. *Annu Rev Ecol Evol Syst*. 2008; 39:115–132.
- Klingenberg CP. MorphoJ: an integrated software package for geometric morphometrics. *Mol Ecol Resour*. 2011; 11:353–357. [PubMed: 21429143]
- Klingenberg CP, Nijhout HF. Genetics of fluctuating asymmetry: a developmental model of developmental instability. *Evolution*. 1999; 53:358–375.

- Lande R. Quantitative genetic analysis of multivariate evolution, applied to brain: body size allometry. *Evolution*. 1979; 33:402–416.
- Le Roith D, Bondy C, Yakar S, Liu JL, Butler A. The somatomedin hypothesis: 2001. *Endocr Rev*. 2001; 22:53–74. [PubMed: 11159816]
- Lieberman DE, Pearson OM, Mowbray KM. Basicranial influence on overall cranial shape. *J Hum Evol*. 2000; 38:291–315. [PubMed: 10656780]
- Marroig G. When size makes a difference: allometry, life-history and morphological evolution of capuchins (*Cebus*) and squirrels (*Saimiri*) monkeys (Cebinae, Platyrrhini). *BMC Evol Biol*. 2007; 7:20. [PubMed: 17300728]
- Marroig G, Cheverud JM. A comparison of phenotypic variation and covariation patterns and the role of phylogeny, ecology, and ontogeny during cranial evolution of New World monkeys. *Evolution*. 2001; 55:2576–2600. [PubMed: 11831671]
- Martin MA, Serradas P, Ramos S, Fernández E, Goya L, Gangnerau MN, Lacorne M, Pascual-Leone AM, Escrivá F, Portha B, Alvarez C. Protein-caloric food restriction affects insulin-like growth factor system in fetal Wistar rat. *Endocrinology*. 2005; 146:1364–1371. [PubMed: 15576465]
- Miller JP, German RZ. Protein Malnutrition Affects the Growth Trajectories of the Craniofacial Skeleton in Rats. *J Nutr*. 1999; 129:2061–2069. [PubMed: 10539785]
- Mitteroecker P, Bookstein FL. The evolutionary role of modularity and integration in the hominoid cranium. *Evolution*. 2008; 62:943–958. [PubMed: 18194472]
- Mitteroecker P, Bookstein FL. The conceptual and statistical relationship between modularity and morphological integration. *Syst Biol*. 2007; 56:818–836. [PubMed: 17934997]
- Mitteroecker P, Gunz P, Bookstein FL. Heterochrony and geometric morphometrics: a comparison of cranial growth in *Pan paniscus* versus *Pan troglodytes*. *Evol Dev*. 2005; 7:244–258. [PubMed: 15876197]
- Monteiro LR. Multivariate regression models and geometric morphometrics: The search for causal factors in the analysis of shape. *Syst Biol*. 1999; 48:192–199. [PubMed: 12078640]
- Morriss-Kay GM, Wilkie AOM. Growth of the normal skull vault and its alteration in craniosynostosis: insights from human genetics and experimental studies. *J Anat*. 2005; 207:37–653.
- Nijhout HF. The nature of robustness in development. *BioEssays*. 2002; 24:553–563. [PubMed: 12111738]
- Nijhout HF. The control of growth. *Development*. 2003; 130:5863–5867. [PubMed: 14597569]
- Oyhenart EE, Muñe MC, Pucciarelli HM. Influence of intrauterine stress on corporal and craniofacial development and sexual dimorphism. *Growth Dev Aging*. 1998; 52:115–122.
- Oyhenart EE, Orden B, Fucini MC, Muñe MC, Pucciarelli HM. Sexual dimorphism and postnatal growth of intrauterine growth retarded rats. *Growth Dev Aging*. 2003; 67:73–83. [PubMed: 14535535]
- Pavlicev M, Cheverud JM, Wagner GP. Measuring morphological integration using eigenvalue variance. *Evol Biol*. 2009; 36:157–170.
- Perez SI, Monteiro LR. Non-random factors in modern human morphological diversification: a study of craniofacial variation in southern South American populations. *Evolution*. 2009; 63:978–993. [PubMed: 19055678]
- Perez SI, Lema V, Diniz-Filho JAF, Bernal V, Gonzalez P, Gobbo D, Pucciarelli HM. The role of diet and temperature in shaping cranial diversification of South American human populations: an approach based on spatial regression and rate tests. *J Biogeog*. 2011; 38:148–163.
- Pigliucci, M. Phenotypic plasticity: beyond nature and nurture. Baltimore, MD, USA: Johns Hopkins University Press; 2001.
- Pigliucci, M. Studying the plasticity of phenotypic integration in a model organism. In: Pigliucci, M.; Preston, K., editors. Phenotypic integration. Studying the ecology and evolution of complex phenotypes. New York: Oxford University Press; 2004. p. 155-175.
- Pigliucci M, Hyden K. Phenotypic plasticity is the major determinant of changes in phenotypic integration in *Arabidopsis*. *New Phytol*. 2001; 152:419–430.

- Pucciarelli HM. The effects of race, sex, and nutrition on craniofacial differentiation in rats. A multivariate analysis. *Am J Phys Anthropol.* 1980; 53:359–368. [PubMed: 6781357]
- R Development Core Team. R Foundation for Statistical Computing. Vienna, Austria: 2008. R: a language and environment for statistical computing. <http://www.R-project.org>
- Ritz, C.; Streibig, JC. *Nonlinear Regression with R.* New York: Springer; 2008.
- Roff D. The evolution of the G matrix: selection or drift? *Heredity.* 2000; 84:135–142. [PubMed: 10762382]
- Rohlf FJ, Slice DE. Extensions of the Procrustes Method for the optimal superimposition of landmarks. *Syst Zool.* 1990; 39:40–59.
- Salazar-Ciudad I, Jernvall J, Newman SA. Mechanisms of pattern formation in development and evolution. *Development.* 2003; 130:2027–2037. [PubMed: 12668618]
- Schlichting CD. Phenotypic integration and environmental change. *Bioscience.* 1989a; 39:460–464.
- Schlichting CD. Phenotypic plasticity in Phlox. II. Plasticity of character correlations. *Oecologia.* 1989b; 78:496–501.
- Sperber, GH. *Craniofacial development.* Hamilton: BC Decker Inc; 2001.
- Stanton ML, Roy BA, Thiede DA. Evolution in stressful environments. I. Phenotypic variability, phenotypic selection, and response to selection in five distinct environmental stresses. *Evolution.* 2000; 54:93–111. [PubMed: 10937187]
- Thissen JP, Keteslegers JM, Underwood LE. Nutritional regulation of the insulin-like growth factors. *Endocr Rev.* 1994; 15:80–101. [PubMed: 8156941]
- Wagner GP. A comparative study of morphological integration in *Apis mellifera* (Insecta, Hymenoptera). *Z Zool Syst Evolut Forsch.* 1990; 28:48–61.
- West-Eberhard, MJ. *Developmental plasticity and evolution.* New York: Oxford University Press; 2003.
- Willmore KE, Leamy L, Hallgrímsson B. Effects of developmental and functional interactions on mouse cranial variability through late ontogeny. *Evol Dev.* 2006; 8:550–567. [PubMed: 17073938]
- Willmore KE, Young NM, Richtsmeier JT. Phenotypic variability: its components, measurement and underlying developmental processes. *Evol Biol.* 2007; 34:99–120.
- Young RL, Badyaev AV. Developmental plasticity links local adaptation and evolutionary diversification in foraging morphology. *J Exp Zool (Mol. Dev. Evol.).* 2010; 314B:434–444.

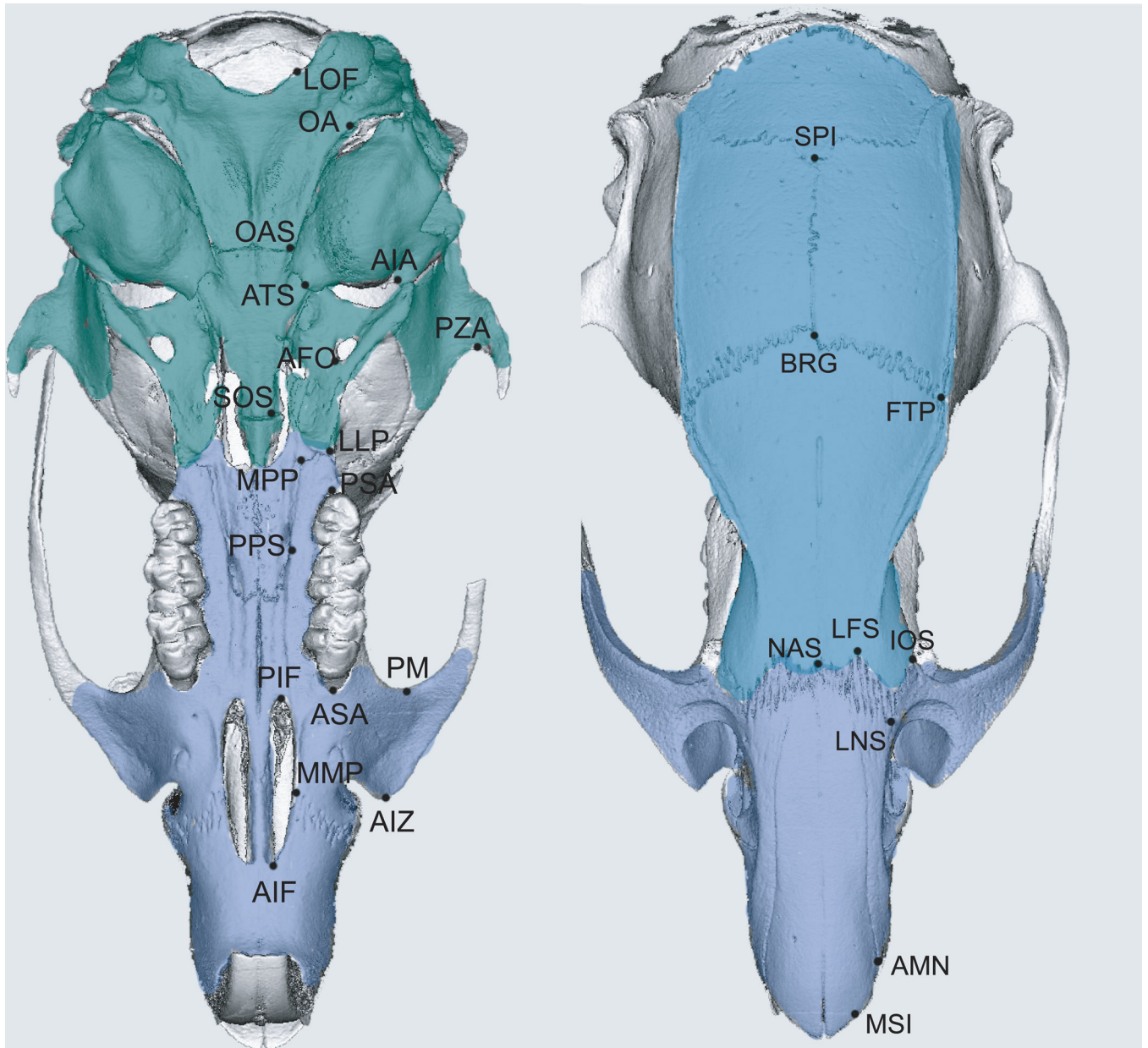


Fig. 1. 3D landmarks collected from rat skull from basicranial and superior views. Landmarks are only shown for one side of the skull; however, landmarks were digitized bilaterally. We show the three components in which the skull was divided: base (green), face (violet) and vault (blue).

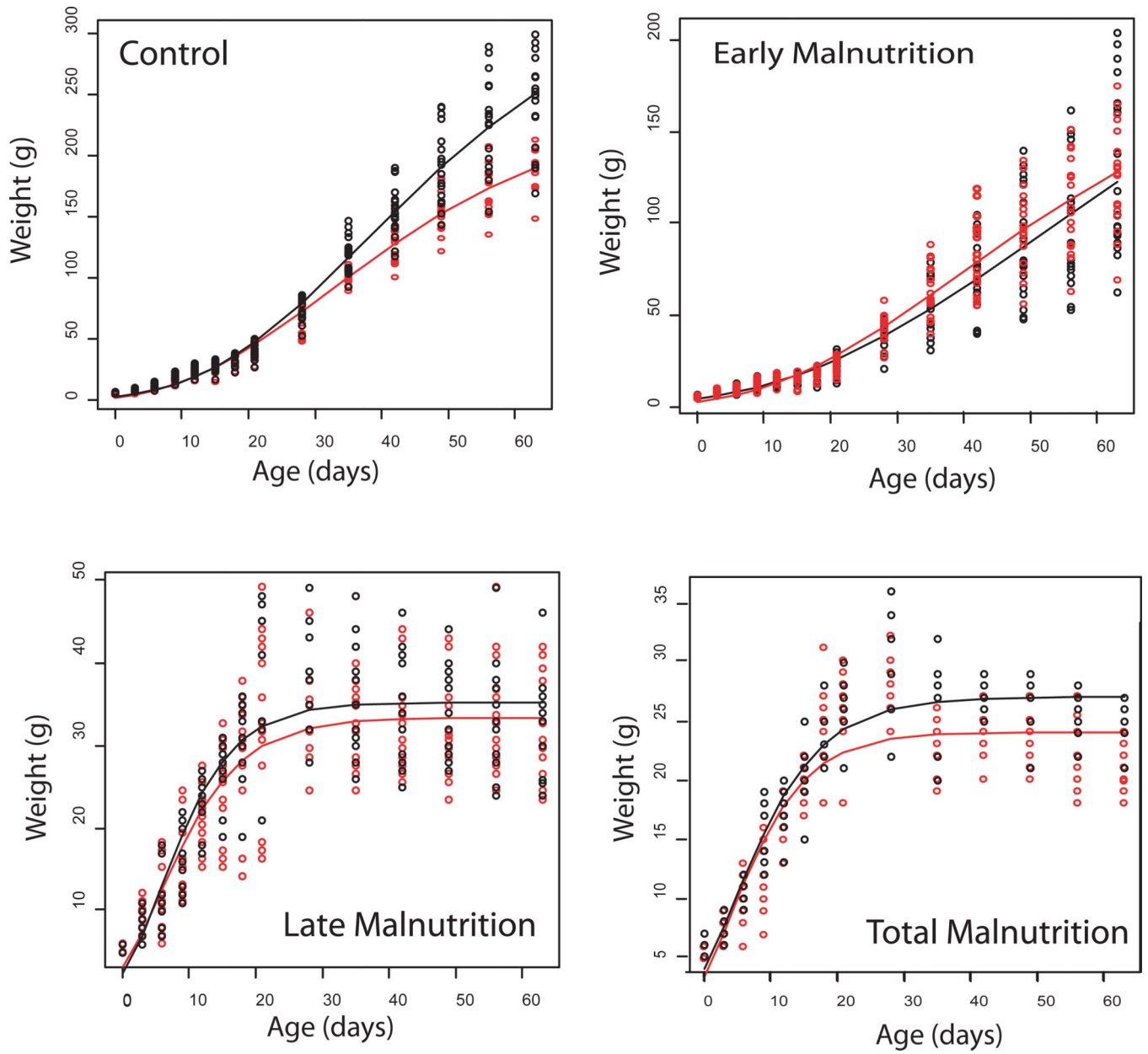


Fig. 2. Longitudinal data for body weight and the adjusted Gompertz model by treatment and sex (Red=female; Black=male).

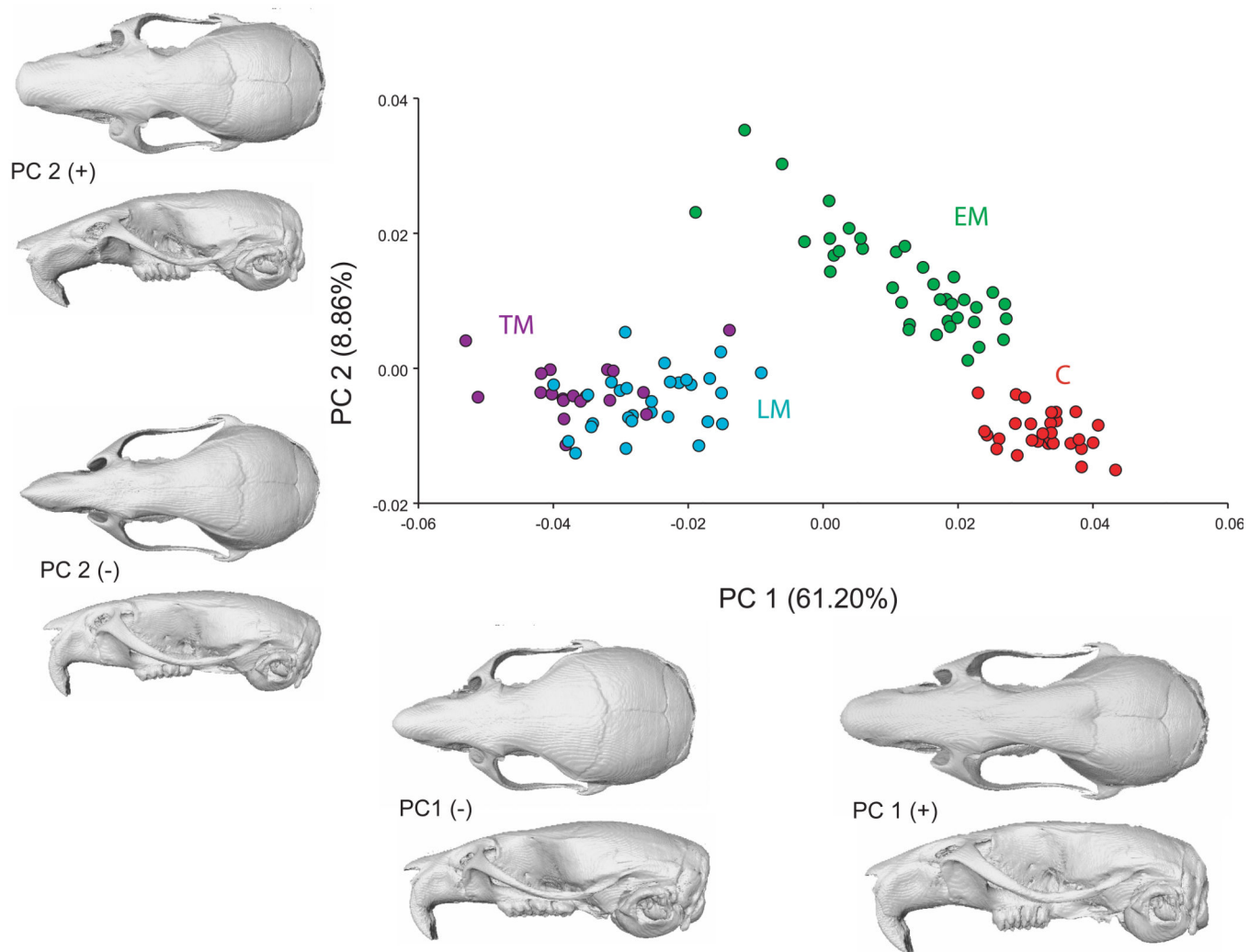


Fig. 3. PCA analysis comparing the distribution of shape variables of the whole skull for the four experimental groups: Early Malnutrition (EM), Late Malnutrition (LM) and Total Malnutrition (TM). For each PC, the shape changes corresponding to the observed extremes in the positive and negative directions are shown as a warped surface of a rat skull (Wiley et al. 2005).

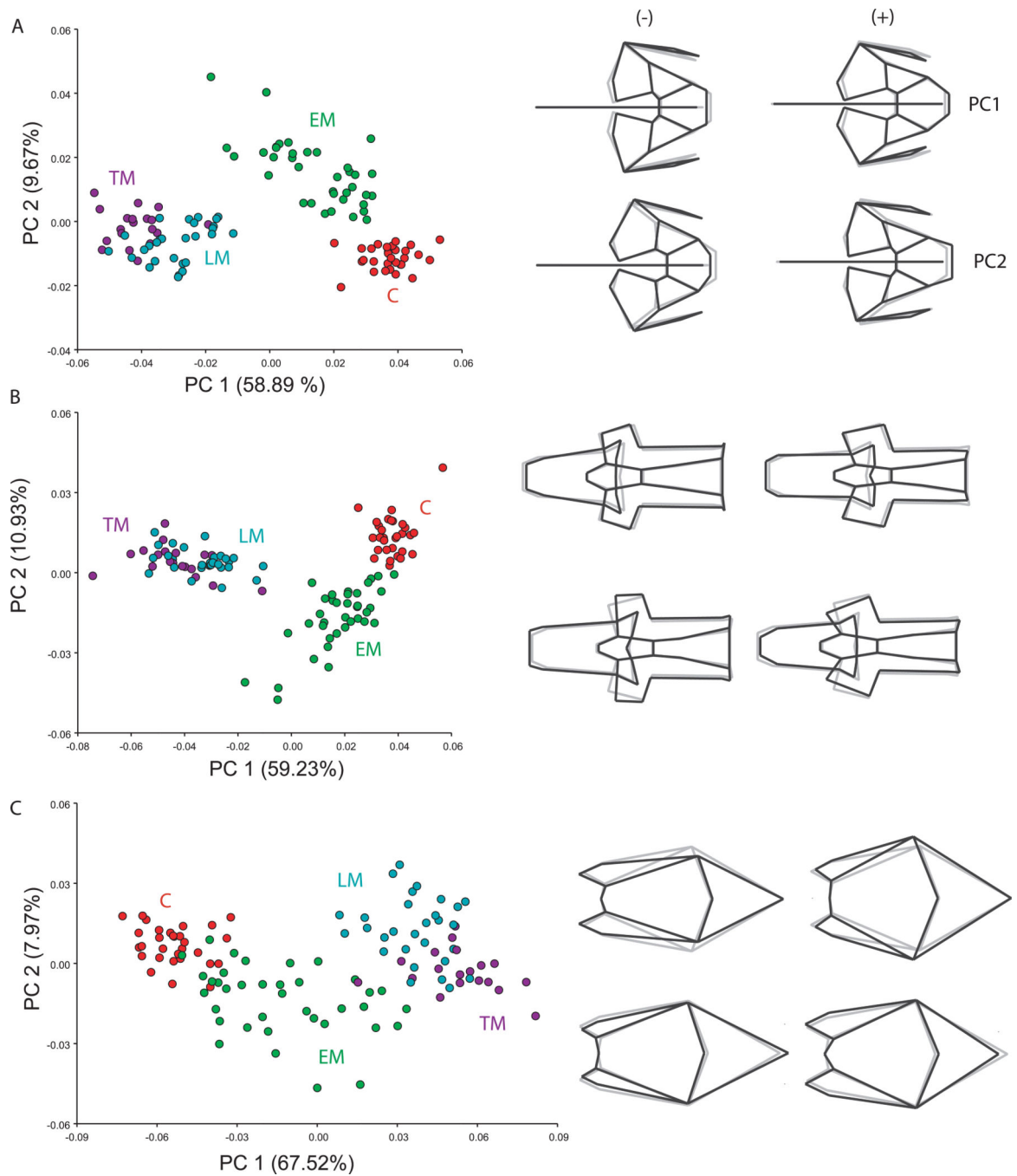


Fig. 4. PCA analysis comparing distributions of shape variables of the base (A), face (B) and vault (C). Wireframes show landmark displacements along PC1 and PC2 for each module. Early Malnutrition (EM), Late Malnutrition (LM) and Total Malnutrition (TM).

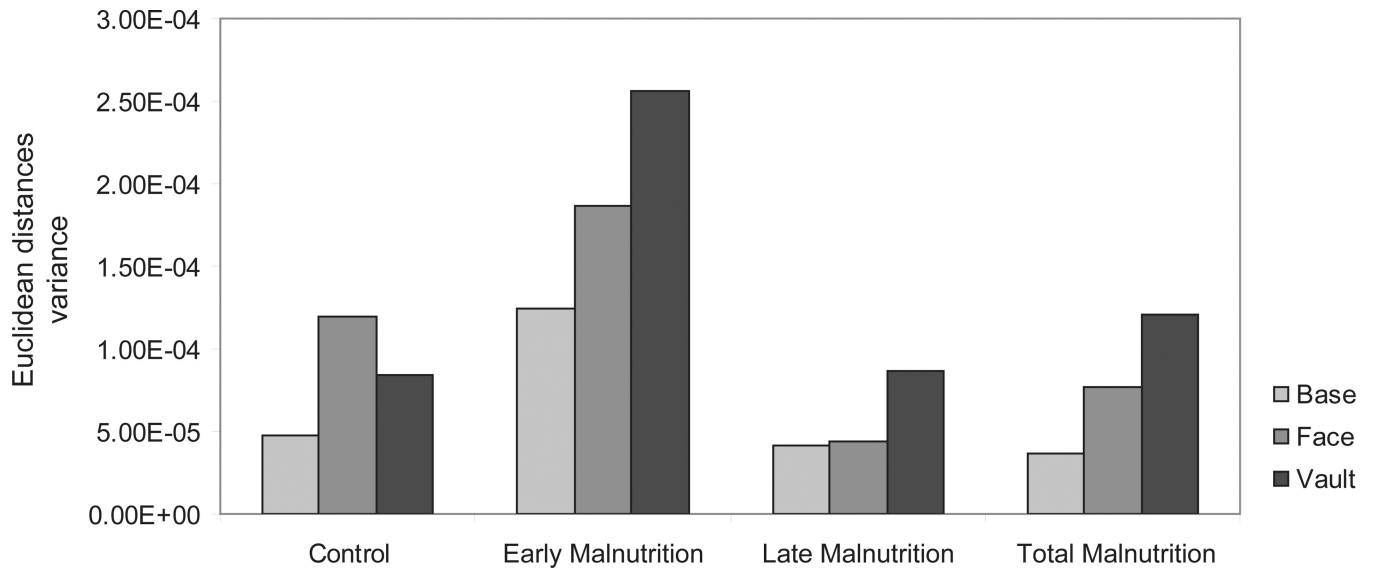


Fig. 5. Within group variance in shape estimated in base to the Euclidean distances along the entire set of PC scores.

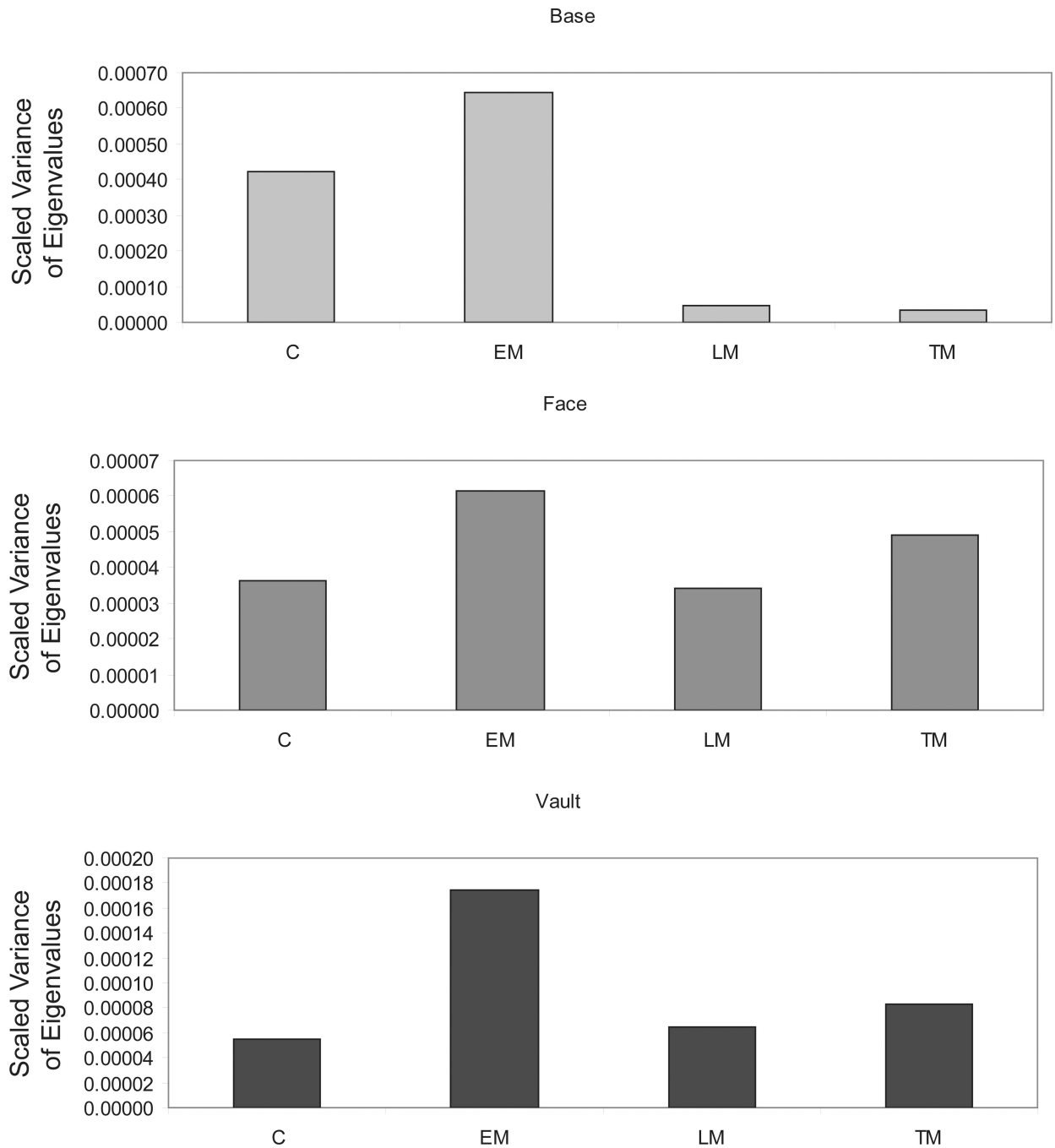


Fig. 6. Variance of eigenvalues for each module of the skull for Procrustes superimposed data. The variances of eigenvalues were scaled by the total variance within each module and group. Control (C), Early Malnutrition (EM), Late Malnutrition (LM) and Total Malnutrition (TM).

Table 1

List of 3D landmarks digitized from rat skulls.

| Landmark Name | Landmark Anagram |
|--|------------------|
| Midline superior incisor | MSI |
| Anteriormost margin of incisive foramen | AIF |
| Anterior inferior zygomatic | AIZ |
| Point of greatest curvature on the posterior margin of the malar process | PM |
| Anterior superior alveoli | ASA |
| Posterior incisive foramen | PIF |
| Point along palatine-maxillary suture | PPS |
| Posterior superior alveoli | PSA |
| Lateral palatal-pterygoid junction | LPP |
| Lateral spheno-occipital synchondrosis | SOS |
| Anterior foramen ovale | AFO |
| Anterior inferior auditory bulla | AIA |
| Point of greatest curvature along posterior edge of zygomatic process of temporal bone | PZA |
| Occipital-auditory-sphenoid junction | OAS |
| Occipital-auditory junction | OA |
| Lateral point on the ventral margin of the occipital foramen | LOF |
| Auditory-temporal-sphenoid junction | ATS |
| Medial palatal-pterygoid junction | MPP |
| Medial maxilla-premaxilla junction | MMP |
| Anteriormost point along lateral zygomatic-frontal suture. | LNS |
| Nasion | NAS |
| Lateral point along frontal suture | LFS |
| Intersection of frontal suture with orbital rim | IOS |
| Frontal-temporal-parietal junction | FTP |
| Bregma | BRG |
| Intersection between the two parietals and the interparietal bone. | SPI |
| Point along occipital-mastoid suture | MST |
| Superoposterior extremity of tympanic ring | TYM |
| Posterior zygomatic-frontal junction | PZF |
| Anterior nasal – premaxilla junction | AMN |
| Medial internal occipital foramen | MOF |
| Medial internal spheno-occipital synchondrosis | MSO |
| Medial internal basi-presphenoid junction | MBP |
| Medial internal anterior point on presphenoid bone | MAP |
| Point on the top of the <i>crista galli</i> | CL |

Table 2

Mean body weight at 63 days old and maximum body weight estimated by the Gompertz model. Confidence intervals (95%) obtained by bootstrap are also given.

| GROUP | Females | | | Males | | |
|---------------------|----------------------|----------------------------|----|----------------------|----------------------------|----|
| | Mean (g) | Asymptote | N | Mean | Asymptote | N |
| Control* | 176.800 | 227.462 213.041–246.610 | 15 | 246.111 | 354.867 321.148–397.394 | 18 |
| Early Malnutrition | 127.158 [†] | 195.352 165.029–244.778 | 19 | 121.864 [†] | 264.511 178.573–581.042 | 20 |
| Late Malnutrition | 30.354 [†] | 32.572 31.476–33.752 | 18 | 32.412 [†] | 35.236 33.927–36.693 | 13 |
| Total Malnutrition* | 20.903 [†] | 23.955 23.199–24.696 | 12 | 25.875 [†] | 27.134 26.239–28.191 | 8 |

^(†) significantly different from Control group;

^(*) group with significant differences between females and males.

Table 3

Mean centroid size and variance of skull components per group. The percentage (%) of reduction in size compared to Control group is also shown.

| GROUP | N | Base | | | Vault | | | Face | | |
|--------------------|----|--------|----------|----|--------|----------|----|--------|----------|----|
| | | Mean | Variance | % | Mean | Variance | % | Mean | Variance | % |
| Control | 30 | 39.385 | 1.138 | - | 26.426 | 0.739 | - | 44.947 | 2.397 | - |
| Early Malnutrition | 38 | 36.439 | 2.636 | 8 | 23.843 | 1.165 | 12 | 41.271 | 4.010 | 7 |
| Late Malnutrition | 27 | 33.069 | 0.412 | 16 | 22.222 | 0.275 | 16 | 36.343 | 0.669 | 19 |
| Total Malnutrition | 20 | 32.063 | 0.700 | 18 | 21.505 | 0.312 | 20 | 34.876 | 0.160 | 23 |

Table 4

Covariance matrix similarity for each pairwise treatment comparison, derived from the set of landmarks of the three modules analyzed separately.

| Anatomical Unit | Groups | Correlation between covariance matrices | | |
|-----------------|--------|---|----------|----------|
| | | Maximum | Observed | Adjusted |
| Base | C-EM | 0.905 | 0.352 | 0.389 |
| | C-LM | 0.892 | 0.379 | 0.424 |
| | C-TM | 0.886 | 0.417 | 0.470 |
| | EM-LM | 0.907 | 0.341 | 0.375 |
| | EM-TM | 0.901 | 0.365 | 0.406 |
| | LM-TM | 0.888 | 0.495 | 0.557 |
| Face | C-EM | 0.901 | 0.335 | 0.372 |
| | C-LM | 0.893 | 0.283 | 0.317 |
| | C- TM | 0.896 | 0.289 | 0.323 |
| | EM-LM | 0.905 | 0.308 | 0.340 |
| | EM- TM | 0.909 | 0.287 | 0.316 |
| | LM- TM | 0.9 | 0.638 | 0.709 |
| Vault | C-EM | 0.885 | 0.430 | 0.486 |
| | C-LM | 0.848 | 0.538 | 0.634 |
| | CI- TM | 0.859 | 0.391 | 0.455 |
| | EM-LM | 0.891 | 0.643 | 0.722 |
| | EM- TM | 0.903 | 0.649 | 0.719 |
| | LM- TM | 0.865 | 0.638 | 0.738 |

Control (C), Early Malnutrition (EM), Late Malnutrition (LM) and Total Malnutrition (TM)

Table 5
 Comparison of integration levels measured by the variance of eigenvalues (λ) and the relative variance of eigenvalues.

| Group | Base | | Face | | Vault | |
|--------------------|---------------------------|-----------------------|---------------------------|-----------------------|---------------------------|-----------------------|
| | observed SD (λ) | rel. SD (λ) | observed SD (λ) | rel. SD (λ) | observed SD (λ) | rel. SD (λ) |
| Control | 3.474E-08 | 7.392E-10 | 2.785E-10 | 5.925E-12 | 1.174E-09 | 5.105E-11 |
| Early Malnutrition | 7.292E-08 | 1.551E-09 | 6.669E-10 | 1.419E-11 | 6.851E-09 | 2.979E-10 |
| Late Malnutrition | 4.023E-10 | 8.560E-12 | 2.464E-10 | 5.243E-12 | 1.522E-09 | 6.618E-11 |
| Total Malnutrition | 2.761E-10 | 5.875E-12 | 4.234E-10 | 9.008E-12 | 2.046E-09 | 8.894E-11 |

Table 6

A pairwise comparison between regression vectors of Procrustes coordinates on centroid size.

| | Treatments | r | Angle |
|--------------|------------|-------|---------|
| Base | C-EM | 0.650 | 49.156 |
| | C-LM | 0.014 | 89.198* |
| | C-TM | 0.330 | 70.731* |
| | EM-LM | 0.513 | 59.136 |
| | EM-TM | 0.754 | 41.062 |
| | LM-TM | 0.555 | 56.289 |
| Face | C-EM | 0.471 | 61.901 |
| | C-LM | 0.039 | 87.765* |
| | C-TM | 0.244 | 75.877* |
| | EM-LM | 0.468 | 62.095 |
| | EM-TM | 0.595 | 53.487 |
| | LM-TM | 0.513 | 59.136 |
| Vault | C-EM | 0.630 | 50.950 |
| | C-LM | 0.656 | 49.004 |
| | C-TM | 0.600 | 53.130 |
| | EM-LM | 0.743 | 42.012 |
| | EM-TM | 0.726 | 43.448 |
| | LM-TM | 0.828 | 34.106 |

Control (C), Early Malnutrition (EM), Late Malnutrition (LM) and Total Malnutrition (TM);

(*) Angles not significantly different from the expected right angle for pairs of random vectors.